PROTEINS: Structure, Function, and Genetics 8:44–61 (1990)

Crystallographic Refinement of Human Serum Retinol Binding Protein at 2Å Resolution

Sandra W. Cowan,[1] Marcia E. Newcomer,[2] and T. Alwyn Jones[1]
[1]Department of Molecular Biology, Biomedicum Centre, S-751 24 Uppsala, Sweden; [2]Department of Biochemistry, School of Medicine, Vanderbilt University, Nashville, Tennessee 37232-0146

ABSTRACT **Human serum retinol binding protein (RBP) in complex with retinol has been crystallographically refined to an R-factor of 18.1% with 2Å resolution data. The protein topology results in an anti-parallel β-barrel that encapsulates the retinol ligand. A detailed description of the protein and the binding site is provided. Our structural work has helped to define a family of proteins, many of which are carrier proteins for smaller ligand molecules. We describe the structural basis for the conservation of sequence within the family.**

Key words: RBP, RBP family, protein structure

INTRODUCTION

Vitamin A (retinol) is an essential nutrient involved in biological processes that include vision, spermatogenesis, and the maintenance of epithelial tissue. Except for its role in vision, the precise mechanism by which retinol fulfills its functions is unclear. However, recently it has been suggested that the retinoids can function as mediators of cell differentiation in a manner similar to that for the steroid hormones.[1] The validity of this hypothesis has recently been demonstrated by the discovery of a nuclear receptor which binds retinoic acid and regulates gene expression.[2,3]

Dietary retinol is ingested as retinyl esters or β-carotene and stored in the liver until its mobilization for the various target tissues. The specific carrier protein for retinol, the retinol binding protein (RBP), is synthesized in the hepatocytes, where it accumulates until the binding of its ligand triggers its secretion.[4,5] Circulating in the plasma, RBP is found bound to transthyretin (previously referred to as thyroxine-binding prealbumin). The formation of this protein complex prevents the lower molecular weight retinol binding protein from being filtered through the kidney glomeruli.[6] Upon delivery of the retinol, however, the RBP-transthyretin complex dissociates[7] and the RBP is filtered and degraded.

On the basis of our structural work,[8] it became clear that RBP is a member of a super-family of proteins defined by a weak sequence homology.[9–11] This family has expanded rapidly[12,13] to include a number of proteins involved in ligand transport. Structural data is available for two other members of the family, β-lactoglobulin[14,15] and bilin binding protein,[16,17] and both show striking structural similarity to RBP.[10,18] Specific cellular carrier proteins for retinol (cellular retinol binding proteins, CRBP and CRBPII) and retinoic acid (cellular retinoic acid binding protein, CRABP) have been characterized.[19,20] These proteins are highly homologous to each other but are specific for their ligands.[21,22] They are members of another super-family of proteins that includes fatty acid binding proteins (FABP), P2 myelin, and adipocyte P2.[23,24] Structures have been determined for two members of this family, intestinal FABP[25] and P2 myelin.[24]

EXPERIMENTAL PROCEDURE

Crystallization and Data Collection

Human RBP was purified from the urine of patients with tubular proteinuria.[26] An extra affinity chromatography step with transthyretin linked to a Sepharose column was made so that only RBP having transthyretin affinity was used for crystallization experiments. Two crystal forms were obtained by the vapor diffusion method by using PEG 6000 and $CdCl_2$ as precipitant in the presence of tris-(hydroxymethyl)aminomethane buffer and 75 mM NaCl.[27] Both forms have the space group $P2_12_12_1$, and we have concentrated on the one with unit cell constants a = 45.7, b = 48.7, c = 76.5Å. These crystals could be grown several millimeters long in the *b* direction but rarely wider than 0.4 mm and 0.25 mm in the *c* and *a* directions, respectively.

The preparations of heavy atom derivatives which were found to produce significant and unique differences were a five hour soak in 5 mM $KAu(CN)_2$ and a 12 hour soak in a 3 mM K_2HgI_4. Data for native and derivative crystals were collected to a resolution of 3.1Å on a Stoe four circle diffractometer at 4°C. The crystals were monitored for decay by measuring standard reflections every 100 reflections. Friedel pairs were collected for both derivatives in blocks of

Received December 18, 1989; revision accepted February 13, 1990.

Address reprint requests to Dr. T. Alwyn Jones, Department of Molecular Biology, Biomedicum Centre, Box 590, S-751 24 Uppsala, Sweden.

TABLE I. Heavy Atom Refinement Data and Statistics*

x	y	z	M	B	R	E
K_2HgI_4						
0.0072	0.2068	0.1196	0.64	30	0.49	2.3
−0.0472	0.2151	0.1320	1.00	36		
−0.0480	0.2352	0.1655	0.67	33		
−0.0844	0.2329	0.1107	0.76	35		
−0.0713	0.1519	0.1470	0.17	35		
$KAu(CN)_2$						
−0.0775	0.2346	0.1105	0.91	33	0.58	1.8

*Overall figure of merit for 2,874 reflections = 0.79. x,y,z = fractional atomic coordinates; M = relative fractional occupancy; B = isotropic temperature factors (Å^2); R = Cullis R-factor; E = $R_{ms}F_h$/Residual.

100 reflections. The Friedel pairs were scaled to each other by using anisotropic scale factors.[28] The native and derivative data were scaled together in shells by the same method.

A 2Å resolution native data set was collected with rotation cameras on Elliott rotating anodes equipped with Franks focusing mirrors[29] and at the Daresbury synchrotron. The films were evaluated on a Vax 750 computer by using a version of the program OSC developed by Rossmann.[30] The 30,316 measurements were scaled and merged by using the PROTEIN system of Steigemann (with the rejection ratios of 0.3 and 0.2. Individual measurements are rejected in PROTEIN if their relative deviation from the mean value exceeds a specified threshhold limit. The two values refer to reflections with more than two measurements and to those with just two measurements.) to give a total of 11,088 reflections with an R_{merge} (with respect to intensities) of 9.0%. This corresponds to 85% of the data to 2Å resolution. At model 62 in the refinement we experimented with different merging methods between the film and diffractometer data sets, using the quality of the retinol electron density as an index of fit. The refinement was continued with a data set made up of the ∞–3.1Å shell from only diffractometer data and the 3.1–2Å shell from film data.

The heavy atom positions were determined by standard difference Patterson and Fourier methods. After several cycles of heavy atom parameter refinement[31] the mercurial site could be resolved into a cluster of five peaks. The final statistics for the refinement are shown in Table I.

Map Interpretation

An electron density map was calculated by using the "best" phases[32] and plotted on plastic sheets to a scale of 3.5 mm per Å. A representative portion of the 3.1Å MIR map showing density for all-trans retinol is shown in Figure 1a and after crystallographic refinement in Figure 1b. The 3.1Å resolution map showed good solvent-protein boundaries, the clear presence of a single α-helix, and extensive β-strands. All map interpretation was carried out on a Vector General 3400 computer graphics system by using a version of FRODO[33,34] adapted to investigate the use of skeletonised electron density. An initial skeletonized version of the MIR map was prepared from the mini-map by the selection of a set of points such that the line joining the points passed through a continuous stretch of electron density. These guide positions were chosen to be approximately 4Å apart and tentative alpha carbons if there were suggestive side chain bulges in the density. This skeleton, when viewed on the computer graphics system, gave a much simplified version of the electron density and greatly helped in testing new connectivity hypotheses. The twist in the β-strands and the hand of the α-helix were immediately seen to be correct.

The normal FRODO commands allowed us to move our skeleton atoms into new positions, create new bonds between them, and generate symmetry-related positions. New commands allowed us to save and restore connectivity hypotheses and to match the amino acid sequence to visual estimates of the size of the density. The latter proved useful in aligning runs of about five residues. This option had no capability for treating insertions and deletions in the alignment.

Peptide oxygens were not usually visible in the map and so could not help in defining the chain direction. The final chain trace accounted for residues 1 to 174, an all trans retinol molecule and the correct set of disulphide bridges (4–160, 70–174, 120–130). The C-terminal residues 175–182 could not be located in the electron density map.

The complete model was constructed from this fold by using guide atoms. For each residue, we positioned the Cα, peptide oxygen (mostly from the local secondary structure), and a side chain atom. The rest of the atoms could be produced as described by Jones[34] and then refitted in the normal way.

Refinement

The course of the crystallographic refinement is outlined in Figure 2. The initial refinement consisted of a number of cycles of reciprocal space least-squares refinement followed by computer graphics refitting by using FRODO. We used the strategy of running CORELS[35] (with each amino acid as a flexible group, connected to adjacent residues by soft restraints) initially at low resolution to remove the largest errors in the model, and subsequently increasing the resolution to 2Å. Since CORELS is a constrained/restrained refinement program, this method induces a build-up of stereochemical errors in the links joining peptide groups. These errors are best smoothed out by using restraints with the high resolution data. Therefore, from model M21–M105 we used PROLSQ.[36]

At this stage of the refinement the first three res-

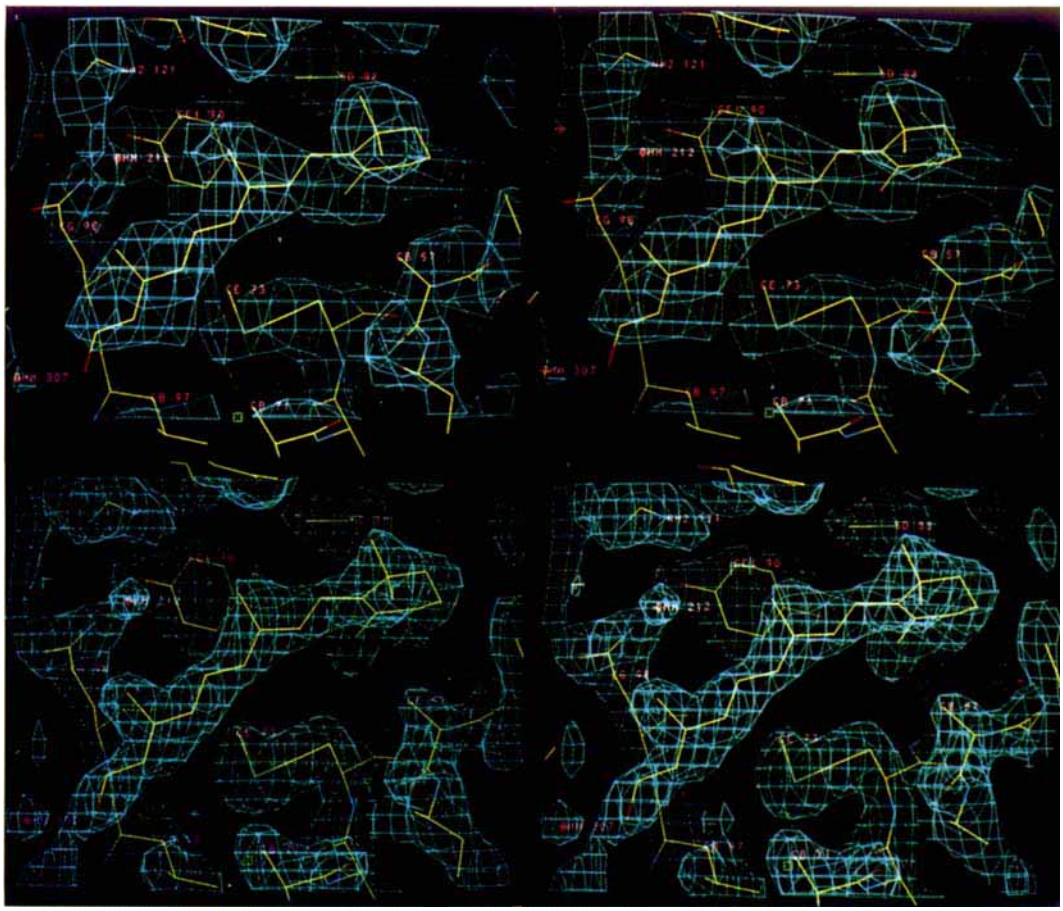

Fig. 1. Electron densities around the retinol binding site: **Top:** the original 3.1Å MIR map and **Bottom:** the final map calculated with (2 $|F_o|-|F_c|$) amplitudes and final model (M116) phases.

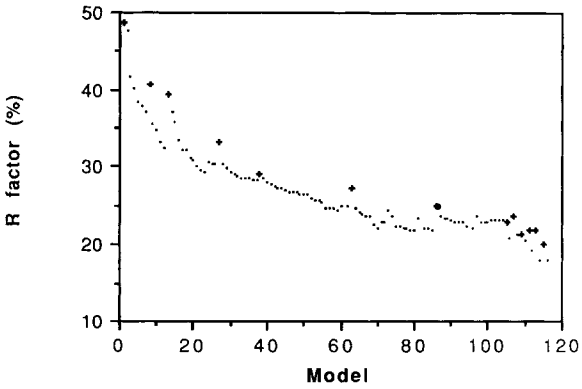

Fig. 2. Crystallographic refinement of RBP. Corels was used from Model 3–7 at 3.1Å resolution, 9–12 at 2.5Å, and 14–20 at 2Å. Prolsq was used from Model M21 to M105 and X-plor from M106 to M116. All manual refitting was carried out with FRODO, Or O, and is marked with +.

idues of the structure and the loop at residue 65 were poorly defined and no new density appeared for the missing C-terminal residues. We therefore carried out several cycles of molecular dynamics refinement with X-Plor.[37] Although this improved the loop 65 region, we were unable to extend the chain past the disulphide at 174.

Quality of the Model

The final model, M116, consists of coordinates and temperature factors for residues 3 to 174 of the sequence as published by Rask et al.,[38] 153 water molecules and a retinol molecule. No density for a cadmium atom was identified. The r.m.s. errors in bond lengths, angles, and fixed torsion angles are 0.014Å and 3.1 and 1.2 degrees, respectively. The crystallographic R-factor is 18.1% for data in the range 8.0–2.0Å.

The real space residue residual factors (Jones et al., to be published) are plotted in Figure 3. This function evaluates for main chain and for side chain atoms of each residue the grid function:

$$\frac{\sum|\rho_{obs} - \rho_{calc}|}{\sum|\rho_{obs} + \rho_{calc}|}$$

where ρ_{obs} is the experimental map and ρ_{calc} is calculated from the model coordinates on the grid of the experimental map. For main chain atoms this plot

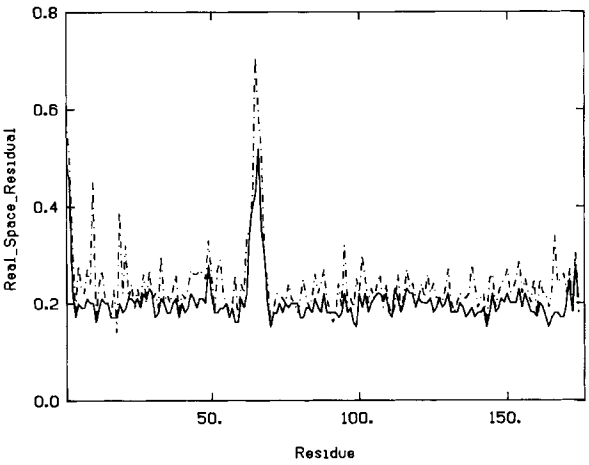

Fig. 3. Real space residual factors for main chain (solid line) and side chain (dashed line) atoms using a 0.8Å grid, three-grid atomic radius, and an overall temperature of 20Å^2.

demonstrates the quality of chain connectivity, while for side chains it can help locate where the sequence is out of register with the density. Only residues 65–66 show poor fitting to the final density.

To locate errors in the orientation of peptide planes, we compare each peptide with a protein data base of refined structures. We use a window of five residues and monitor the r.m.s. deviation of the carbonyl oxygen of the center residue to the best-fitting data base peptides. During refinement we carefully check all residues where this value is greater than 2.5Å. In the final model only four residues deviate with values greater than 2.5Å (at residues 21, 39, 171, and 33). All of these peptide oxygens correspond to clusters having multiple conformations, frequently with a glycine in one cluster and a non-glycine in the other. In all cases, the electron density is unequivocal. The distribution of main chain torsion angles[39] is shown in Figure 4a and plotted in Figure 4b.[40] Only Y111 falls outside the normal allowed regions for non-glycine residues.

All structural comparisons are made using the O program (Jones et al., to be published). As one of its features the program allows one to obtain a transformation matrix relating two molecules or parts of molecules. This matrix can then be refined. This algorithm attempts to first find the longest fragment where, after superposition, each pair of atoms in the fragment fits better than a certain value after alignment (3.8Å). This is repeated until a minimum fragment length is reached (four residues). The matching pairs of atoms are then used to calculate a new transformation matrix and the process is continued until covergence is reached.

Secondary structural elements and turns are defined by the program DSSP.[41]

DESCRIPTION OF THE MOLECULE

RBP consists of a single globular domain of approximately 40Å in diameter that almost totally encapsulates the retinol molecule as shown in Figure 5. The main chain hydrogen bonds are given in Figure 6. This figure also shows the surface area accessible to a water molecule for each amino acid in the protein and residues whose accessible surface area changes upon removal of the retinol molecule. Of the three disulphide bridges, one covalently links the N-terminal region to the C-terminal end of the α-helix (4–160), the second joins the last visible residue to the β-barrel (70–174), and the third link is between the two neighboring anti-parallel strands (120–129). The secondary structural elements and turns are listed in Table II.

The N-terminal region, Figure 7, is both highly charged (ten charges in the first nineteen residues) and highly conserved within RPB's.[43] Residues 1 and 2 have no interactions with other parts of the protein but are located near the C-terminal region of a symmetry related molecule. Peptides 6–8 and 17–19 each form a turn of 3_{10} and α helices, respectively. There are few other main chain to main chain hydrogen bonds in this region.

Residues which contribute to the formation of the retinol containing barrel start at residue 12. The methylene groups of the lysine side chain of K12 help close off the barrel while the imido group salt links to D13. Another salt link, K17 to D79, helps seal the barrel (Fig. 7). Of the large hydrophobic residues in this region two (F15, F20) point into the barrel and one (F9) is in the interface between the helix-sheet packing.

The principal feature of the β-barrel core is the eight anti-parallel β-strands (A–H) that fold with a simple $(+1)_7$ topology. The main chain hydrogen bonding scheme shown in Figure 6 results in the formation of two orthogonal β-sheets. This is achieved by some strands being shared between the two sheets.[44] The front sheet in Figure 5 is made of strands A–F, while the back sheet is made up of EGFHA and I (where strand I is from the C-terminal region around 167). The sharing of strand A between the two sheets is achieved by a β-bulge at A26–M27. This is similar to the classic bulge described by Richardson[45] but M27 and K29 hydrogen bond to strand I rather than B. The other principal shared strand, F, is distinctly banana shaped allowing it to take part in both sheets although its hydrogen bonding to strand G is disturbed by a bulge between V107 and D108. The strand curvature thus allows a smooth change from the front sheet to the back sheet whilst maintaining the hydrogen bonding pattern.

The folding topology results in two possible entrances/exits to the barrel that are made up from loop residues between adjacent strands (Figs. 7, 8).

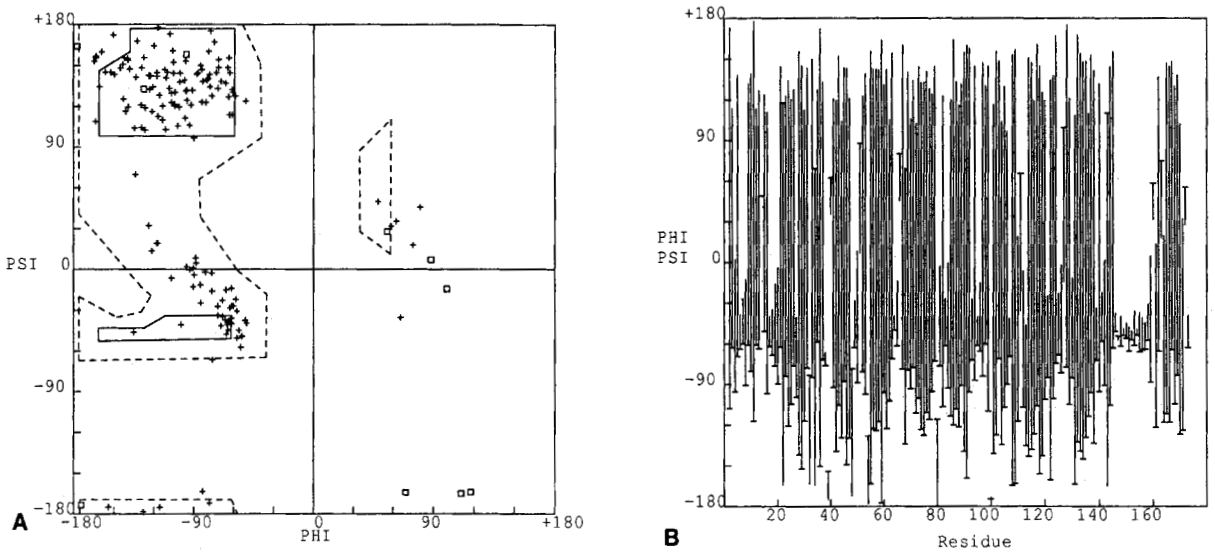

Fig. 4. **A:** Distribution of main chain dihedral angles for RBP. Glycines are plotted with □, non-glycines by +. The preferred regions of Ramakrishnan and Ramachandran[39] are indicated. **B:** Main chain dihedral angles plotted as described by Balusubramanian.[40] The ϕ and ψ values for each residue are represented by a vertical line so that the horizontal bar is the ϕ angle.

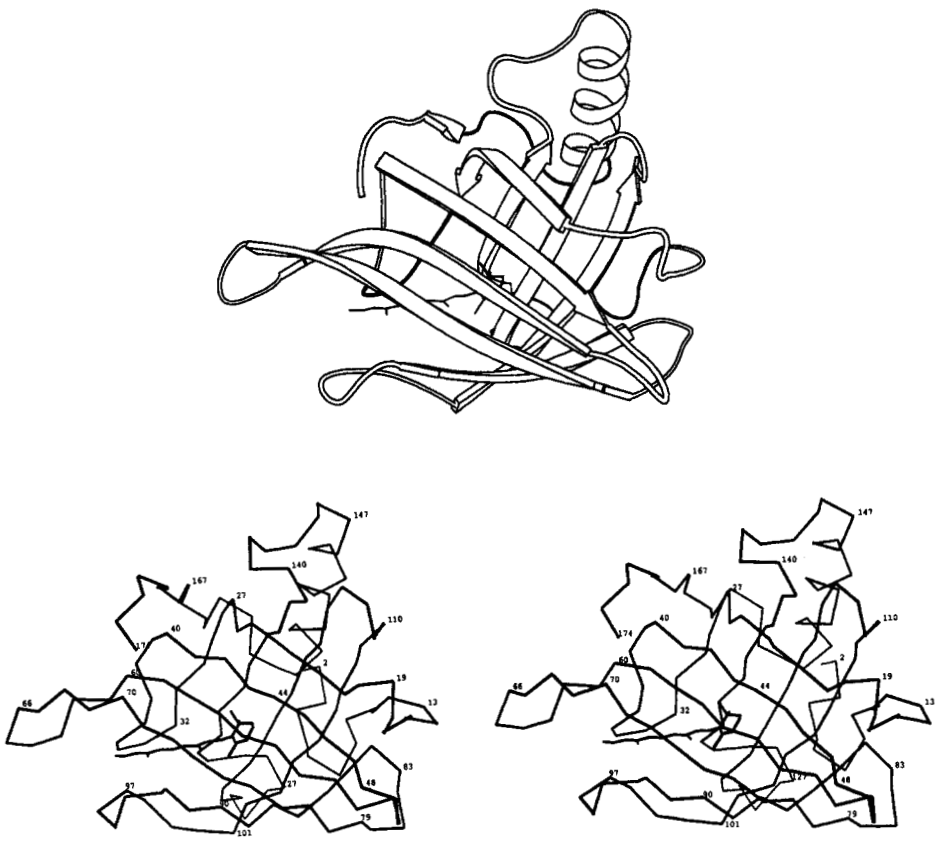

Fig. 5. Cα plot of RBP with bound retinol. The view is chosen to show the orthogonal β-sheets. The ribbon drawing was prepared with a program written by Priestle.[100]

The hairpin conformations are included in Table II. Figure 8 shows that in the first loop, strands A and B are rather separated. Because of the secondary structure, the side chain of K29 should point into the barrel. Instead the side chain twists the imido group out into solution, forming a salt bridge to D31. A

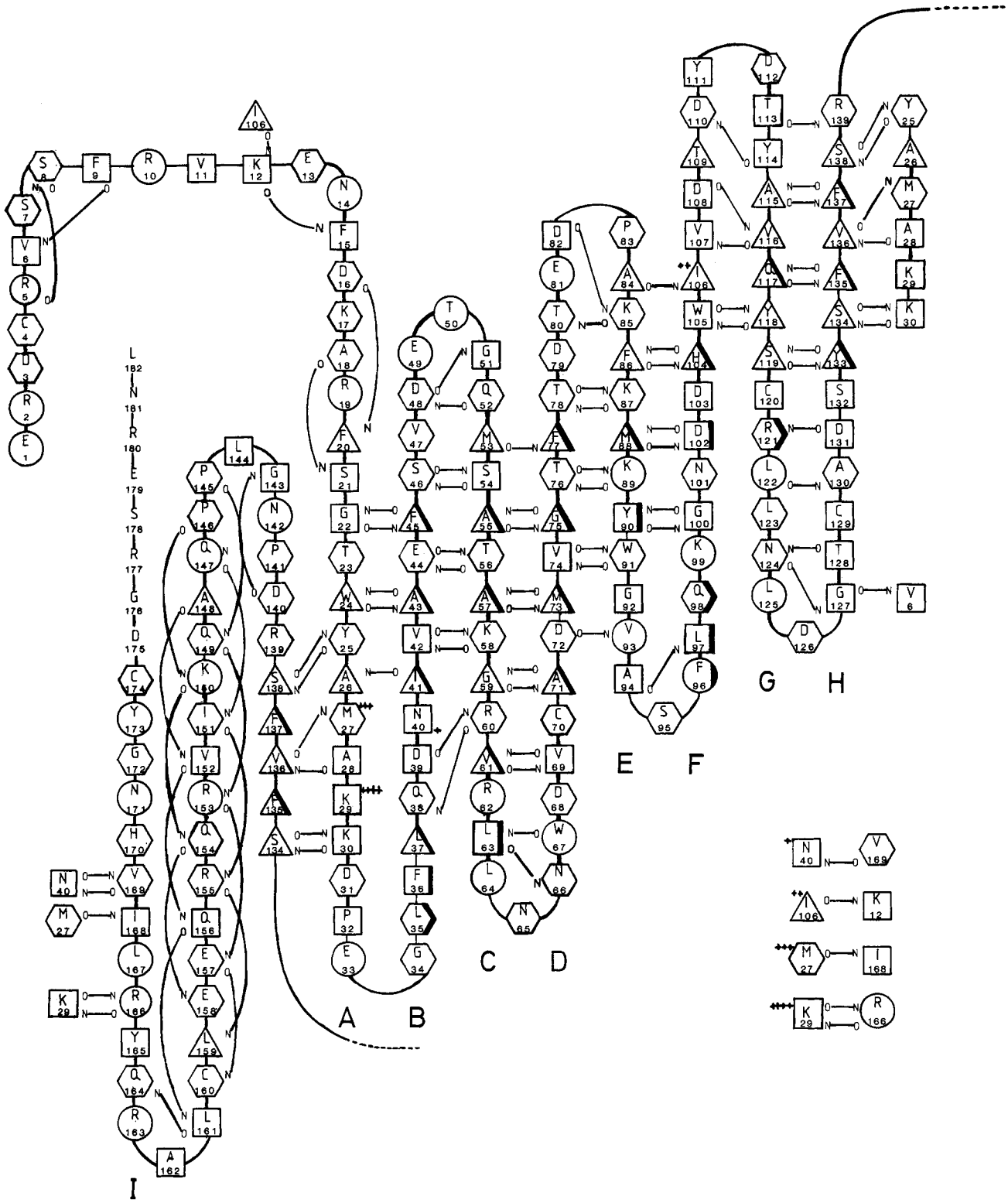

Fig. 6. Schematic of the amino acid sequence and H-bonding pattern for RBP. The geometric shape indicates the accessible surface area of each amino acid. A circle indicates substantial accessible surface area (>100Å^2), a hexagon slightly less (40–100Å^2), and a square even less (5–40Å^2). A triangle indicates a minimal amount of accessible surface area (0–5Å^2). Those shapes which contain a thickened line enclose the amino acids which have a change in accessible surface area upon the removal of retinol.

TABLE II. Secondary Structure According to the Algorithm of Kabsch and Sander[41]*

Secondary structure	Amino acids
β-strand A	22–30
β-strand B	39–47
β-strand C	53–62
β-strand D	68–78
β-strand E	85–92
β-strand F	100–109
β-strand G	114–123
β-strand H	129–138
β-strand I	166–167
α-helix	146–158
DSSP Hairpin assignments	
31–38	ββββεββββα
48–52	βα$\gamma_R\gamma_L$β
63–67	βα$\gamma_R\gamma_L$β
79–84	ββγ_Rβ$\gamma_R\gamma_R$
93–99	αβααββββ
110–113	$\gamma_R\gamma_L\gamma_R\alpha$
124–128	βα$\gamma_R\gamma_L$β

*The symbols used to describe the conformations of residues in the hairpins are: α for α-helix, β for β-strand, α_L for left handed α-helix, and ε for residues having φ, ψ values close to (70, −120), γ_L and γ_R having values close to (± 90, 0), respectively. This is based on the nomenclature used by Efimov.[42]

distinctive 'hump' in the chain is achieved before the start of strand B by N40 adopting an α_L conformation.

Two of the hairpin bends in the barrel (between BC and GH) are identical. This is a very common turn,[46] with a distinctive split hydrogen bonding pattern (Fig. 6). It consists of a type I turn (48–51 and 124–127) with a bulge (51 and 127). This gives a strong glycine preference at a location corresponding to residues 51 and 127 where the residue adopts a left-handed α-helix conformation.

The DE hairpin is less common but a similar conformation occurs in dihydrofolate reductase[47] where both structures have a proline in equivalent positions (P83 and P148 respectively).

In the sixth hairpin (FG), Y111 adopts a non-standard conformation. This is a conserved structural feature in the RBP family of proteins and is discussed in more detail in a later section.

The disulphide bond formed between C120 and C129 crosses between the two anti-parallel strands G and H (Fig. 8). Richardson[45] points out that it is not possible to join neighboring strands in an ideal β-sheet since the closest pair of residues is slightly too close and the rest are too far away. However, in RBP there are matching discontinuities in the strands, at R121 and A130 respectively, so that the H-bond ladder pattern becomes out of step with respect to the start of the strands. This causes a change in direction of approximately 70° such that the Cα separation of C120 and C129 is only 5.9Å. The eighth and final strand of the barrel is regular from D131–R139 and is terminated by a type III turn (D140–G143).

The four-turn helix packs onto one of the β-sheets with an angle of approximately −15°, the value commonly observed for the packing of α-helices on β-sheets.[48] The extensive interactions, Figure 9, are continuous along the helix with Y114, V136, L144, A148, and V152 in one hydrophobic cluster at the top half of the helix and V107, V116, L159, L161, Y118, and the hydrophobic part of R155 (salt-linked to D108) at the C-terminus of the helix. At the base of the helix, the chain makes a type I turn to pass back across the barrel and form the C7—C174 disulphide bond. Residues 165–170 have a β-stand-like conformation and form H-bonds to strands A and B.

The C-terminal residues D175–L182 were not visible in the isomorphous replacement map and did not appear during the refinement.

Internal Sequence Homology

Rask et al.[49] identified an internal repeat in the amino acid sequence of human RBP. This repeat is not evident in the gene sequence.[50] Peptides F36–P83 and F96–P141 have 34% identity when two insertions are allowed (Fig. 10). These repeats form strands BCD and FGH and their structures can be roughly superimposed by a two-fold rotation around the barrel axis. In fact, by starting with only the β-sheet hydrogen bonding residues, strands A–D can be superimposed on E–H with an r.m.s. deviation of 1.63Å for 35 paired Cα atoms (Fig. 11). Seven of the 16 repeated amino acids are found in the loop regions R62–D72 and R121–D131, which splay in opposite directions. The inserted residues E49 and G75 occur in a loop and in the middle of a β-strand, respectively. The latter insertion (G75) in the β-strand is not compensated for by the formation of a beta-bulge.

The repeated peptides comprise three quarters of the β-barrel and therefore not too surprisingly contribute most of the residues which line the retinol binding site. Only one homologous pair, F77 and F137, is structurally conserved in the superposition. This is the only pair where both residues contribute to the retinol binding site.

The Retinol Binding Site

The retinol molecule is completely encapsulated by the β-barrel core, with the β-ionone ring in the center and the isoprene chromophore stretching along the barrel axis almost to the solvent surface. The van der Waals surfaces of the protein and the retinol are highly complementary. Removal of the retinol from the model leaves a deep invagination stretching into the center of the barrel (Fig. 12).

Residues whose accessible surface area changes upon removal of the retinol molecule are highlighted in Figure 6 and also drawn in Figures 12 and 13. The binding of retinol reduces the accessible surface area[51] of the holo-RBP structure by 251Å^2 and the accessible surface area of the retinol itself by

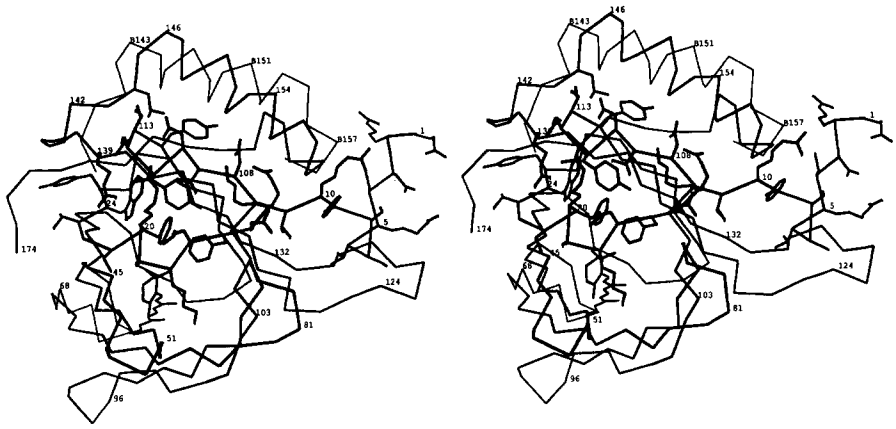

Fig. 7. Loop regions at the "closed" end of the RBP barrel and the N-terminus. The helix from BBP is also drawn after applying the transformation relating their barrels. Some of the residues whose sequences are conserved in the RBP family are also drawn (W24–R139, Y25–P141, L144, T109–D110–Y111–D113–Y114).

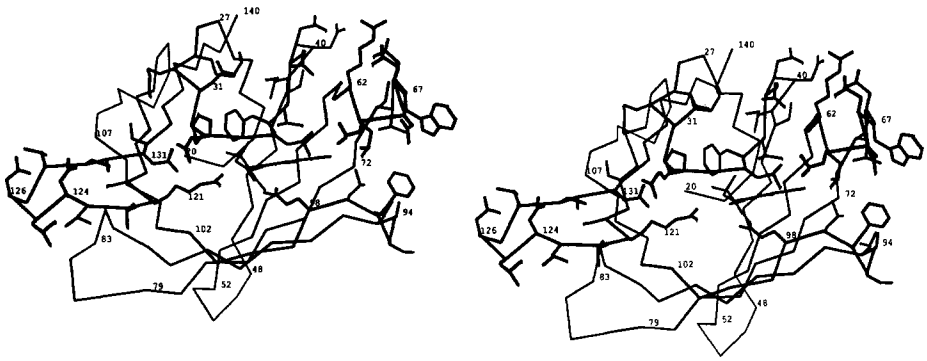

Fig. 8. Loop regions at the barrel entrance/exit.

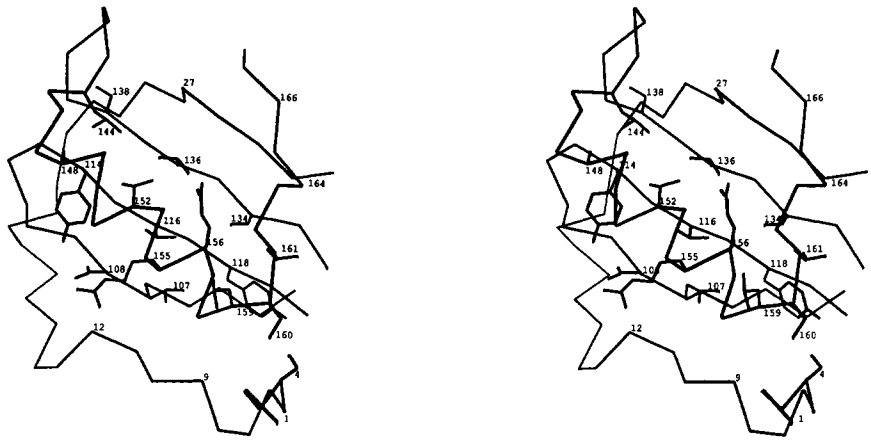

Fig. 9. Helix-β-sheet packing in RBP.

551Å^2. The accessible surface area of retinol in holo-RBP is 1Å^2 (at O21). For comparison, this net loss of accessible surface area corresponds to the area lost per subunit upon dimer formation in the satellite tobacco necrosis virus capsid.[52]

The retinol can enter the barrel from just one end.

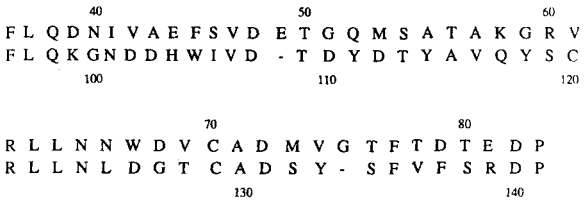

Fig. 10. Internal sequence homology.

The other end of the barrel is blocked by five phenylalanine rings (15, 20, 45, 77, 86) and a methionine (53) (Fig. 12). The phenylalanine rings are evenly spaced with their ring center about 5Å from the sulphur atom of M53. Neighboring phenylalanine rings are stacked perpendicularly to each other, except for F77, which stacks perpendicular to the ring of H104. This arrangement of hydrophobic side chains is shielded from the solvent by the salt link K17 to D79.

The β-ionone ring is displaced slightly from the barrel axis (Fig. 8) due to an asymmetric size distribution of the neighboring residues. The ring fits between the Cβ atoms of A43, A55, and A57 from one sheet and Y133, F135, and H104 from the other. The other residues around the β-ionone ring are F45, M88, and M73. The residues forming the binding pocket for the isoprene tail are V61, Q98, L37, M73, L35, Y90, and F36. The closest contacts are shown schematically in Figure 13. Solvent 212 hydrogen bonds with the side chain of Q98 and R121 while a second solvent 181 hydrogen bonds to the side chain of H104 and Y133 (Fig. 12). Arg 121, by forming a salt link to D102 helps close off the entrance. Residues Q98 and L35 could control the entrance/exit to the barrel. Changing their side chain conformation would open up the binding site to solvent (or receptor.) The closest contacts to the retinol alcohol group are CD2 of L35, CD2 of L97, CD2 of L63 and solvent 307, forming a hydrogen bond. The initial MIR map was not good enough to unambiguously define the orientation of the β-ionone ring relative to the isoprene tail. However, the plane of the β-ionone ring became clear during the refinement (cf. Figure 1a and 1b). The conformation of the β-ionone ring relative to the isoprene tail is determined by the dihedral angle defined by the C5-C6-C7-C8 atoms (Fig. 13). This angle is 62° in the final model. Table III shows this dihedral angle for a number of retinoids as determined from their coordinates deposited at the Cambridge Data Bank. Clearly preferred values of ±60° and 180° exist. These results are in agreement with spectroscopic data. The retinol absorption spectrum shows little or no shift, and no fine structure when bound to RBP[6,53] suggesting that the conformation of the retinol in the binding site is equivalent to the solution conformation.

Various in vitro studies on the binding of retinoids and related compounds to apo-RBP suggest that RBP may be able to accommodate a variety of retinol analogs. In addition to retinol, the protein binds retinoic acid[54,55] with a dissociation constant comparable to that of retinol (2.1×10^{-7} M vs. 1.9×10^{-7} M).[56] Horowitz and Heller[55] reported that the absorption spectrum of retinoic acid bound to RBP was reversibly pH dependent, suggesting that the carboxyl group is available to the solvent. The accessible surface shown in Figure 12 clearly suggests this possibility. Simply replacing the functional end group with a carboxyl group causes a very close contact to L35. Because the retinoid is so long, a small pivotal rotation of the isoprene tail at C6 can reduce this close contact without making poor contacts around the β-ionone ring. Q98 may be in a position to interact with this carboxylate.[57]

The ability of RBP to bind all trans retinaldehyde has been demonstrated by a number of laboratories.[54–56] In addition, the aldehyde group of the retinal molecule is accessible to small inorganic ions, as in situ RBP-bound retinal can be reduced to retinol.[55] However, the functional group cannot be oxidized by alcohol dehydrogenase (ADH). The above observations are all consistent with the fact that the tail of the retinol reaches to the surface, but is not to any large extent exposed and certainly not exposed enough to enter the active site of ADH, some 15Å from the enzyme's surface.[28]

The 13-cis and 11,13-di-cis isomers of all-trans retinol are also reported to bind to RBP[54] as well as 9-cis, 11-cis, and 13-cis retinaldehyde.[55] Although we have modelled these compounds in RBP, we consider the models to be speculative (and of no biological relevance).

Gawinowicz and Goodman[58,59] report an affinity label for RBP that covalently attaches to the peptide 1–5/156–163. This region is far from our observed binding site but as far as we can judge, appears close to the retinol binding site reported for β-lacto-

TABLE III. C5-C6-C7-C8 Dihedral Angles for Retinoids

Retinoid	Dihedral angle (degrees)	Reference
2,6-Di-cis-4-hydroxyretinoic acid-γ-lactone	48	92
Retinoic acid	42	93
11-cis-retinal	41	94
2-cis-4-hydroxyretinoic acid-γ-lactone	−47	95
Retinyl acetate	−58	96
All-trans retinal	−58	97
13-cis-retinal, second molecule	−65	98
9-ethyl-retinoic acid	−64	99
Retinoic acid	−166	93
13-cis-retinal, first molecule	−175	98

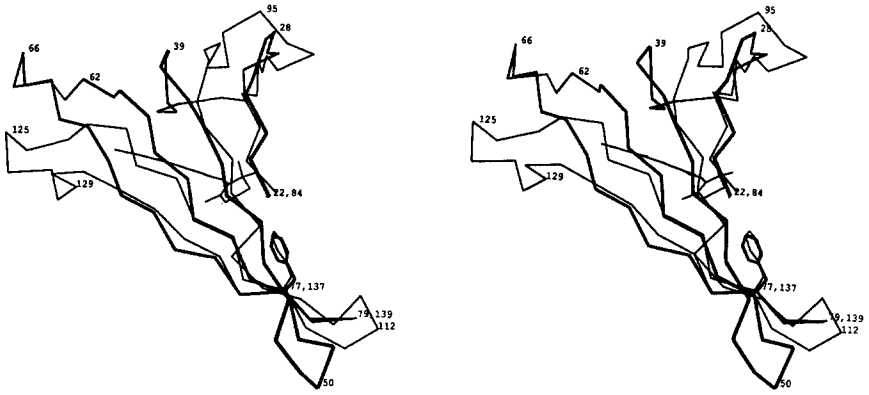

Fig. 11. Superposition of strands A–D, E–H based on the H-bonding ladders.

Fig. 12. The contour net shows the accessible surface available upon removal of the retinol molecule. Residues within 4Å of the retinol are shown (L35, F36, L37, A43, A55, A57, V61, L63, M88, Y90, L97, Q98, F135), together with those closing off the barrel (F15, F20, F45, F77, F86, M53, H104, K17, D79), and some of the residues making conserved interactions within the RBP family (W24–R139, Y25–P141, L144, T109–D110–Y111, Y165, I168).

globulin.[15] The structural solution of a second crystal form of RBP[60,61] should eventually help in deciding on the presence of a second binding site.

A Putative Transthyretin Binding Site

RBP in normal human serum is found complexed with transthyretin (TTR). This complex can be broken up by reducing the ionic strength.[53] Whether or not the apo form has an affinity for transthyretin has been a source of debate in the literature. No TTR binding activity is observed for apo-RBP prepared by repeated ethanol extraction of lyophilized protein.[62] Peterson[63] identified a "free," i.e., non-transthyretin-bound, form of RBP in serum which lacked its ligand. However, RBP isolated from urine by Fex et al.[64] is retinol free and binds to a transthyretin affinity column. When eluting the column by a gradient of decreasing ionic strength, the apo form is released first. Raz and Goodman[65] as well as Rask et al.[66] report that retinol-free RBP prepared by heptane extraction binds to transthyretin, albeit with a lower affinity. The addition of TTR to the extraction experiments impeded the extraction of retinol from RBP.

Chemical modifications suggest the presence of an RBP tryptophan in the TTR-RBP interaction site. Two out of four tryptophans in RBP are modified by the reagent 2-hydroxyl-5-nitrobenzyl bromide.[67] The modification does not affect the binding of retinol to RBP nor does bound retinol afford protection from the reagent. However, the modified RBP does not complex with TTR and the presence of TTR inhibits the reaction with one of the tryptophans.

One would expect the binding sites to be highly conserved across different species: human and chicken RBPs and transthyretins actually cross-interact.[68] This led us to suggest the N-terminus of the molecule and C-terminal base of the α-helix, which is the best conserved region in RBP, as a possible transthyretin binding site. Of the four tryptophan residues in RBP, two are buried (24 and 105) and two are exposed (W67 for which we have poor/no

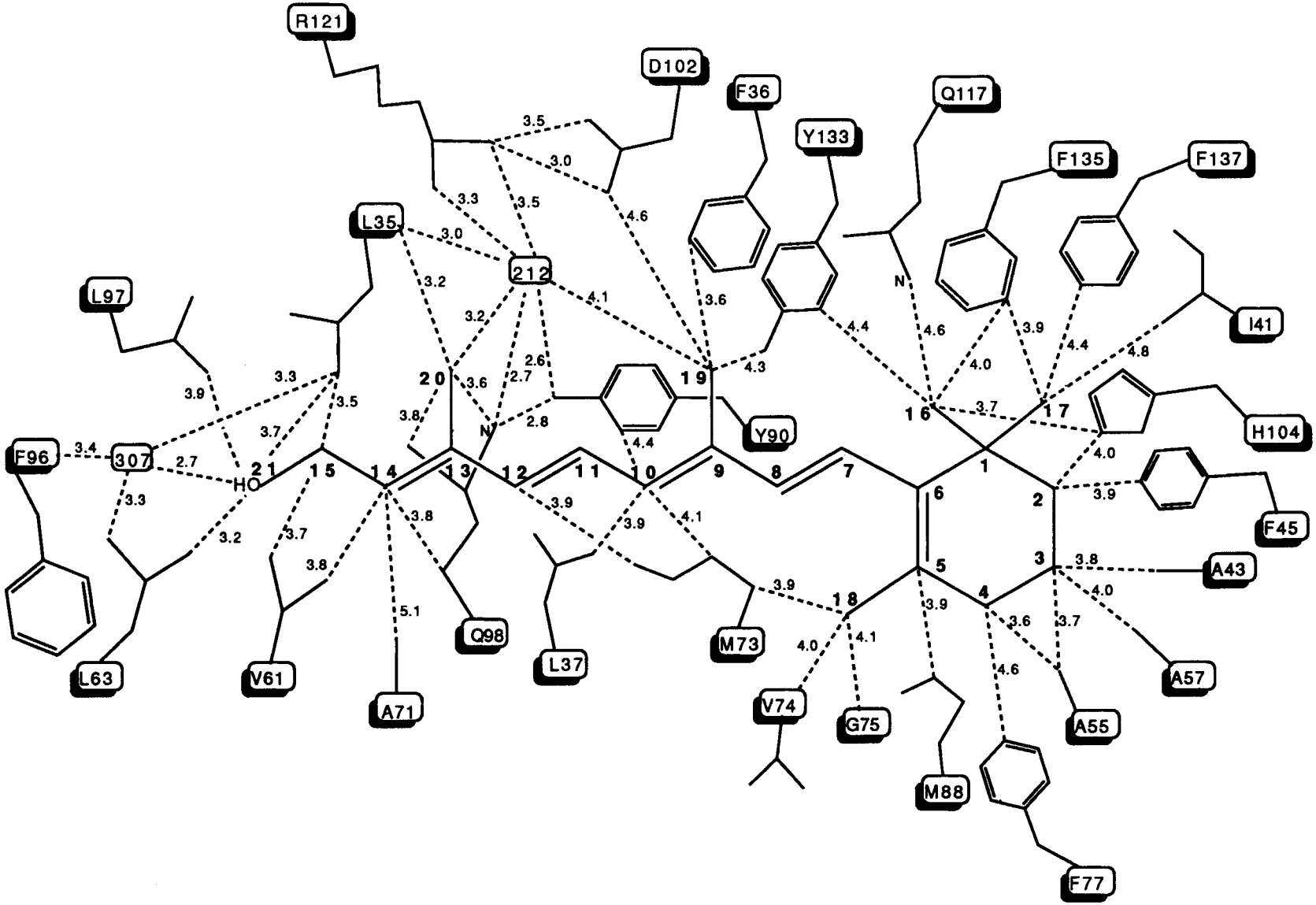

Fig. 13. Retinol numbering and schematic of closest contacts (Å).

density for the side chain, and W91 which is in well defined density). The residues in these loops are therefore more likely to be close to or part of the transthyretin binding site. Both regions have exposed hydrophobic residues (Fig. 6) that could be expected to take part in the binding site. A model which includes extensive hydrophobic interactions would be consistent with the observed dissociation of the RBP/transthyretin complex at low ionic strength.

The conformational changes induced by the removal of retinol have been predicted by molecular dynamics simulations.[69] They suggest a change of conformation in the entrance loops in the apo form with respect to those in the holo form. These changes could result in a reduced affinity of apo-RBP for TTR. The loop region around N65 remains poorly defined in our maps and suggests conformation flexibility. Forming a complex with transthyretin could stabilize the loops in this region and explain why heptane extraction of RBP in the presence of TTR is slowed relative to its extraction from free RBP. This closing of access to the retinol by the docking of TTR is also consistent with the fact that the fluoresence spectra of TTR binding to retinol-RBP indicate an increased hydrophobicity around the chromophore.[70]

These arguments serve as hypotheses that must be tested experimentally. We hope to confirm them by carrying out a crystallographic investigation of the complex.

Structural Similarity With Other Proteins

Dayhoff et al.[71] describe the sequence comparison of bovine β-lactoglobulin and human α1-microglobulin as an example of an alignment near the limit of detection of sequence homology. After determining the sequence of RBP Peterson and coworkers recognised its similarity to these proteins. We therefore suspected the existence of a family of proteins whose function is to solubilise small lipid molecules.[8] Definitive proof required the structure of another member of the family. The bovine β-lactoglobulin structure was solved by Sawyer et al.[14] and by comparing the structures, it was possible to show their great similarity and to locate three short peptides that have sequence identity and are structurally equivalent.[10] The family is characterized by a common motif, where the β-sheets are structurally very similar but with greater variation in some of the connecting loops. The regions with greatest sequence similarity are separated in the sequence but are spatially close to one another.[18] The sequence homology has also been recognized independently by Godovac-Zimmermann et al.[72] and Pervaiz and Brew.[9] The structure of a third member of the family, bilin-binding protein or insecticyanin, has been determined by Huber et al.[16,18] and Holden et al.[17] Huber et al.'s[18] comparison of BBP and RBP strengthens the structural definition of the family. In both RBP and BBP the ligand is located in the center of the barrel. Recently Monaco et al.[15] have solved the structure of the BLG/retinol complex and report that the retinol binds in the α-helix/β-sheet interface. In BBP and RBP, however, the ligands are in structurally equivalent positions in the barrel (Fig. 15).

On the basis of the sequence alignment, the family has now rapidly expanded.[12,13] Most of these proteins bind small hydrophobic ligands. Because of the low sequence homology, the alignments that have been published contain numerous errors. Figure 14 shows a new sequence alignment for RBP: purpurin (PURP), a retina cell adhesion molecule that binds retinol[73]; the insect biliverdin binding protein (BBP),[18] and insecticyanin (INCY)[74] which bind bilin pigments; β-lactoglobulin (BLG),[75] the major protein component of the milk whey of ruminants (and also other animals) which binds a number of hydrophobic molecules, including retinol[76]; apolipoprotein D (APOD),[77] a component of high density lipoprotein in human plasma; α-1-microglobulin (HC) which binds an unknown chromophore[78,79] and is also called protein HC; androgen-dependent secretory protein (ADSP) from rat epididymis[80]; a number of serum proteins: α-2-microglobulin (A2M),[81] the related mouse urinary protein (MUP),[82] and α1-acid glycoprotein (A1AG)[83]; two proteins linked to olfaction: one from frog Bowman glands (OBP1),[84] and the so-called odorant binding protein (OBP2) from nasal epithelium that is known to bind odorants[11]; a human placental protein 14 (PP14), progesterone-dependent pregnancy-associated endometrial α2-globulin[85]; and aphrodisin (APHR), a hamster aphrodisiac protein.[86] Although the overall conservation of residues is low within the family (only W24 is conserved completely), some members are more closely related in sequence. For example, RBP and purpurin have 48% identity with one insertion while RBP and α1-acid glycoprotein have only 7% identity and possibly seven deletions.

After superposition of only the barrels, BBP and RBP can be aligned with an r.m.s. deviation of 1.65Å for 97 CA atoms (Fig. 15). This superposition also causes the alignment of 163–170 (strand I) with the equivalent residues in BBP (Fig. 15). The structurally conserved residues correspond almost exactly to the regular sheet residues. In regions of low homology, therefore, we have resisted introducing extra distortions in the sheet. Although we believe this alignment to be more accurate than those previously published, it still needs to be treated with some caution.

The family shows great variation in the N-terminus region. Aphrodisin is the most truncated, starting with the first residue of RBP that actually protrudes into the barrel. The region at the beginning of the β-barrel is the most highly conserved

```
      A1ag   .QNPEPANI TLGIPITNET LKWLSDKWFY MGAAFRDP.. VFKQAVQTIQ
      Aphr   ......... ........QD FAELQGKWYT IVIAADNLE. .KIEEGGPLR
      Obp2   ......... .AHHENLDIS PSEVNGDWRT LYIVADNVE. .KVAEGGSLR
        Hc   ...GPVPTPP DNIQVQENFN ISRIYGKWYN LAIGSTC... .PLKIMDRMT
       Mup   ........E EASSTGRNFN VEKINGEWHT IILASDKRE. .KIEDNGNFR
       A2m   ........E EASSTRGNLD VAKLNGDWFS IVVASNKRE. .KIEENGSMR
      Adsp   ......... ...AVVKDFD ISKFLGFWYE IAFASKMGTP GLAHKEEKMG
      Obp1       .QCQA DLPPVMKQLE ENKVTGVWYG IAAASNC... .KQFLQMKSD
      Pp14   ........M DIPQTKQDLE LPKLAGTWHS MAMATNNI.. .SLMATLKAP
       Blg   ........L IVTQTMKGLD IQKVAGTWYS LAMAASDI.. .SLLDAQSAP
      Apod   ..QAFHLGKC PNPPVQENFD VNKYLGRWYE IEKIPTTF.. ...ENGRCIQ
      Incy    GDIFYPGYC PDVKPVNDFD LSAFAGAWHE IAKLPLE... .NENQGKCTI
       Bbp     NVYHDGAC PEVKPVDNFD WSNYHGKWWE VAKYPNS... .VEKYGKCGW
      Purp   .....QTCAV DSFSVKDNFD PKRYAGKWYA LAKKDPE... .GLFLQDNIS
       Rbp        ERDCRV SSFRVKENFD KARFSGTWYA MAKKDPE... .GLFLQDNIV
      Dssp        ccccg ggccccttcc ttttceeeee eeeeccs... .scccceeee
    C_Struc              ********* ********** ******.... .....*****
  In barrel              .......b. ...b...b.. .b...b.... ...b....b.
                           |         |         |              |
 RBP number                10        20        30             40

      A1ag   TEYFYLTPNL INDTIELREF QT.TDDQCVY NFTHLGVQRE N.....GTLS
      Aphr   FYFRHIDCYK NCSEMEITFY VI.TNNQCSK TTVIGYLKGN G......TYQ
      Obp2   AYFQHMECGD ECQELKIIFN VK.LDSECQT HTVVGQKHED G......RYT
        Hc   VSTLVLG.EG ATEAEISMTS TRWRKGVCEE TSGAYEKTDT D.....GKFL
       Mup   LFLEQIHVLE NSLVLKFHTV R...DEECSE LSMVADKTEK A.....GEYS
       A2m   VFMQHIDVLE NSLGFKFRIK E...MGECRE LYLVAYKTPE D.....GEYF
      Adsp   AMVVELKENL LALTTTYYSE .....DHCVL EKVTATEGDG P.....AKFQ
      Obp1   NMPAPVNIYS LNNGHMKSST SFQTEKGCQQ MDVEMTTVEK G......HYK
      Pp14   LRVHITSLLP TPEDNLEIVL HRWENNSCVE KKVLGEKTGN P.....KKFK
       Blg   LRVYVEELKP TPEGDLEILL QKWENGECAQ KKIIAEKTKI P.....AVFK
      Apod   ANYSLMENGK IKVLNQELRA D....GTVNQ IEGEATPVNL TEPA...KLE
      Incy   AEYKYDG.KK ASVYNSFVSN GV.....KEY MEGDLEIAPD AKYTKQGKYV
       Bbp   AEYTPEG.KS VKVSNYHVIH G.....KEYF IEGTAYPVGD S...KIGKIY
      Purp   AEYTVEEDGT MTASSKGRVK LFGFWVICAD MAAQYTVPDP TTP...AKMY
       Rbp   AEFSVDETGQ MSATAKGRVR LLNNWDVCAD MVGTFTDTED P.....AKFK
      Dssp   eeeeecttsc eeeeeeeeee ettteeeeee eeeeeeecss t.....teee
    C_Struc  *******.** ********.. .......*** *****..... *.....****
  In barrel  b.b..... b.b.b.b.b. b.....b.b. b.b.b..... ........b.
                 |         |         |         |
 RBP number      50        60        70        80

      A1ag   KCAG...... ..AVKIFAHL IVLKKHGTFM LAFNLT.... .DENRGLSFY
      Aphr   TQFEG..... ..NNIFQPLY ITSDKIFFTN KKNMDRA... .GQETNMIVV
      Obp2   TDYSG..... ..RNYFHVLK KTDDIIFFHN VNVDES.... .GRRQCDLVA
        Hc   YHKSKWN... ..ITMESYVV HTNYDEYAIF LTKKFSRH.. HGPTITAKLY
       Mup   VTYDG..... ...FNTFTIP KTDYDNFLMA HLINEKD... GETFQLMGLY
       A2m   VEYDG..... ...GNTFTIL KTDYDRYVMF HLINFKN... GETFQLMVLY
      Adsp   VTRLS..... ..GKKEVVVE ATDYLTYAII DITSLVA... GAVHRTMKLY
      Obp1   WKMQQG.... ...DSETIIV ATDYDAFLME FTKIQMG... AEVCVTVKLF
      Pp14   INYTV..... ...ANEATLL DTDYDNFLFL CLQDTTT... PIQSMMCQYL
       Blg   IDA....... .LNENKVLVL DTDYKKYLLF CMENSAE... PEQSLACQCL
      Apod   VKFSWFM... ..PSAPYWIL ATDYENYALV YSCTCIIQL. .FHVDFAWIL
      Incy   MTFKFG...Q RVVNLVPWVL ATDYKNYAIN YNCDYHP.DK KAHSIHAWIL
       Bbp   HKLTYG...G VTKENVFNVL STDNKNYIIG YYCKYDE.DK KGHQDFVWVL
      Purp   MTYQGLASYL SSGGDNYWVI DTDYDNYAIT YACRSLKEDG SCDDGYSLIF
       Rbp   MKYWGVASFL QKGNDDHWIV DTDYDTYAVQ YSCRLLNLDG TCADSYSFVF
      Dssp   eeeeesstts cceeeeeeee eecsssseee eeeeeectts seeeeeeeee
    C_Struc  ***..... ....****** ********** *****..... ..*********
  In barrel  b.b......b ..b.b.b.b. .b.....b.b .b.b..... ...b.b.b.b
                 |         |         |         |         |
 RBP number     90       100       110       120       130
```

Fig. 14.

```
          A1ag  AKKPD.LSPE LRKIFQQAVK DVGMD.ESEI VFVDWTKDKC SEQQKQQLEL
          Aphr  GKGNA.LTPE ENEILVQFAH EKKIPV..EN ILNILATDTC PE........
          Obp2  GKRED.LNKA QKQELRKLAE EYNIPN..EN TQHLVPTDTC NQ........
            Hc  GRAPQ.LRET LLQDFRVVAQ GVGIPE..DS IFTMADRGEC VPGEQEPEPI
           Mup  GREPD.LSSD IKERFAQLCE EHGILR..EN IIDLSNANRC LQARE.....
           A2m  GRTKD.LSSD IKEKFAKLCE AHGITR..DN IIDLTKTDRC LQARG.....
          Adsp  SRSLD.DNGE ALYNFRKITS DHGFSE..TD LYILKHDLTC VKVLQSAAES
          Obp1  GRKDT.LPED KIKHFEDHIE KVGLKK..EQ YIRFHTKATC VPK.......
          Pp14  ARVLV.EDDE IMEGFIRAFR PLPRHL.WYL LDLKQMEEPC RF........
           Blg  VRTPE.VDDE ALEKFDKALK ALPMHI.RLS FNPTQLEEQC HI........
          Apod  ARNPN.LPPE TVDSLKNILT SNNIDV..KK MTVTDQVNCP KLS.......
          Incy  SKSKV.LEGN TKEVVDNVLK TFSHLIDASK FISNDFSEAA CQYSTTYSLT
           Bbp  SRSKV.LTGE AKTAVENYLI GSPVV.DSQK LVYSDFSEAA CKVN......
          Purp  SRNPRGL... PPAIQRIVRQ KQEEICMSGQ FQPVLQSGAC ..........
           Rbp  SRDPNGL... PPEAQKIVRQ RQEELCLARQ YRLIVHNGYC DGRSERNLL.
          Dssp  essttcc... chhhhhhhhh hhhhttcttc ceeccccscc
       C_Struc  *****..... ..******** .........** ******....
     In barrel  ......a... a..aa..a.. .a......... a..a
                   |            |          |         |
RBP number         140          150        160       170

          A1ag  EKETKKETKK DP
          Aphr  .......... ..
          Obp2  .......... ..
            Hc  LIPR...... ..
           Mup  .......... ..
           A2m  .......... ..
          Adsp  RP........ ..
          Obp1  .......... ..
          Pp14  .......... ..
           Blg  .......... ..
          Apod  .......... ..
          Incy  GPDRH..... ..
           Bbp  .......... ..
          Purp  .......... ..
           Rbp  .......... ..
```

Fig. 14. Alignment of the RBP family of sequences. The row "DSSP" describes residue assignments where e refers to a β-strand, h to an α-helix, g to a 3_{10} helix, t to a piece of helix normally a turn, s to a bend where the angle between the ($C\alpha_{i-2}$-$C\alpha_i$) and ($C\alpha_i$-$C\alpha_{i+2}$) vectors is greater than 70°, and c is unassigned. In the row "C-struc," "*" marks structurally conserved residues. For residues in the row "In barrel," residues labelled "b" point into the barrel, while "a" residues are in the helix/sheet interface.

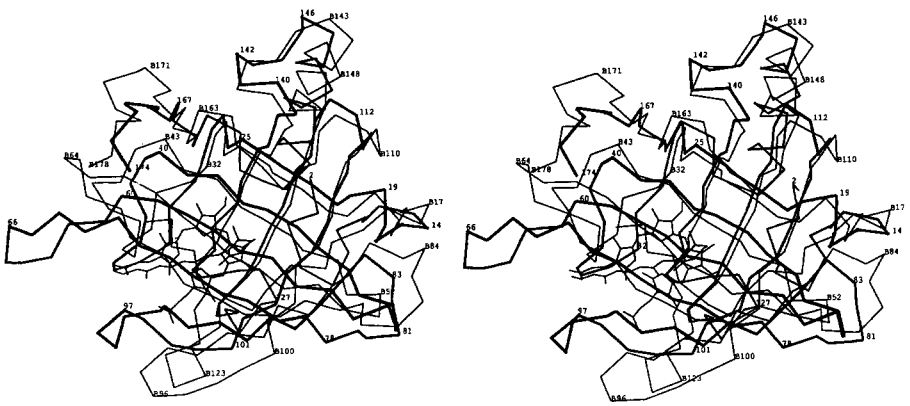

Fig. 15. Structural alignment of RBP and BBP, using the barrel residues to obtain the transformation matrix. The transformation matrix was obtained after limiting the comparison to residues 1–140 in RBP.

sequence in the family, in particular G22 and W24. The conformation shows a strong glycine preference at G22 in our database of refined structures, using a fragment length of five residues. The main chain conformational angles are (118°, −164°) (Fig. 4b). Only rat A1AG has a non-glycine while in human A1Ag, it is a glycine.[87] The tryptophan ring W24 forms a hydrophobic cluster packing with F20, A115, and F137 (Fig. 12). Both 20 and 137 show tendencies for aromatic residues while 115 is usually an alanine or another hydrophobic residue. Only two of the proteins (PP14 and BLG) lack an aromatic in this cluster. The interaction of W24–R139 (Figs. 7, 12) and their conservation in the CRBP family have been described by Jones et al.[24] A similar interaction occurs between K85 and W105 in RBP, where in this case the basic residue is well conserved but the tryptophan is not. The residue at Y25 has a strong tendency for an aromatic side chain. This external residue stacks onto the ring of a well conserved P141 (Fig. 12).

The greatest uncertainties in the alignment occur in strands B and C. In RBP there is a very regular alternation of hydrophobic/hydrophilic residues because of the regular β-sheet structure. In strand B we have tried to preserve an alternating hydrophobic alignment with an aromatic at F45 where possible. The strand C alignment is also based on the "best" alignment of hydrophobic residues pointing into the barrel. The CD hairpin shows much variation in structure but the location of cysteine residue C70 in RBP is conserved both structurally and in the sequences. The next hairpin contains the only insertion/deletion between RBP and purpurin. It is also the location of an insertion in insecticyanin relative to BBP. However, the conserved K85 and F86 make the alignments more reasonable. A larger variation in structure is to be expected at the hairpin connecting E and F. Except for purpurin, all family members have deletions at this hairpain, relative to RBP.

In contrast the next hairpin is highly conserved both in structure and sequence. It has the second best conserved sequence region in the family. The conservation of the triplet T109, D110, Y111 is due to specific hydrogen bonds from these side chains to main chain atoms. T109 is internal (Figs. 7, 12), surrounded by well conserved hydrophobic residues (F15, F20, W24, I106, F137). However 109 OG1 forms hydrogen bonds to 114O and 111N (both 2.8Å). The latter is possible because of the unusual conformation of Y111. D110 also forms two H-bonds, to main chain atoms 113N and 114N (both 2.8Å). Y111 is wedged between the sheet and the residues forming the start of the barrel, its hydroxyl group hydrogen bonding to 16N (3.0Å) (Figs. 7, 12). Residue 114 is either F or Y (except for A1AG), helping to form the helix-sheet interface (Fig. 9).

The next structurally highly conserved residues are R139 and P141 (Figs. 5 and 7), allowing us to backtrack in the alignment to the GH hairpin with a high degree of confidence. Only purpurin has the disulphide linking the two strands G and H. G143 in RBP is an insert (kept in purpurin), while L144 is very highly conserved, pointing into the β-sheet/α-helix interface (Figs. 7, 9). This also forces a small residue at residue 138. The helices are not as structurally conserved as the barrel and we have therefore used just the barrel residues to make the structural alignment of RBP and BBP. The helices are then out of register by about half a turn (Fig. 7). This accounts for the apparently large insertion relative to RBP at L144. Since only purpurin keeps the disulphide from the C-terminus of the helix to the protein N-terminus, the rest of the family has been aligned to BBP. The likely residues packing onto the β-sheet can then be identified. These include a number of arginine and lysine residues that can pack the hydrophobic parts of their side chains onto the sheet as does R155 in RBP (Fig. 9).

The packing of Y165 and I168 onto the barrel (Fig. 12) and the conservation of the 70–174 disulphide allow the assignment at the C-terminus. Note that in BBP/INCY the C-terminal disulphide is the equivalent of N40 in RBP. APOD is most closely related to BBP/INCY in sequence (27% identity to BBP). It also has a cysteine close to N40 but no cysteine close to C70, so we have therefore made its alignment to satisfy the BBP/INCY disulphide bridge.

The similarity between the RBP family and the cellular retinoid/fatty acid binding protein family has been described by Jones et al.[24] Similar architectural principles have been preserved between both families, using a similar kind of strand topology to form the barrel, with the first strand shared by two orthogonal sheets. The cellular family, however, uses ten strands to form the barrel. The only structurally conserved sequence identity is GxW at the start of each barrel. The stacking of a basic side chain onto this tryptophan ring is also conserved.

The eight-stranded β-barrels have also been seen in catalase[88] and streptavidin,[89,90] while the structure of a ten-stranded photoreceptor protein has recently been described.[91] These are clearly not members of the RBP family.

Since many members of this family may react with receptors, possibly in ways depending on the presence or absence of ligand, it is necessary to know the effect of ligand removal on the protein. Removing a ligand, approximately 15Å long, from the center of a small protein may be expected to lead to profound changes in the protein; e.g., the sheets may collapse (our first suggestion, Newcomer et al.[8]). However, the striking structural similarity of RBP to BBP and BLG, of RBP to P2 myelin,[24] and of apo and holo BLG[15] makes it more plausible to suggest that the integrity of the barrel is retained due to the protein architecture, the elegant topology that gives

rise to orthogonal β-sheets. This does not rule out more subtle, local changes that would be sufficient to alter a protein-protein interaction.

ACKNOWLEDGMENTS

We wish to thank Per A. Petersson for stirring our interest in retinol and for supplying us with the material to carry out this study. We would also like to thank Robert Huber for supplying us with BBP coordinates. We are grateful for support from the Swedish Natural Sciences Research Council and the Wallenberg Foundation. M.E.N. also thanks Hoffmann-La-Roche (Basel) for support during some of this study.

The coordinates have been deposited at the Protein Data Bank, Brookhaven, for immediate distribution.

REFERENCES

1. Green, S., Chambon, P. A superfamily of potentially oncogenic hormone receptors. Nature 324:615–617, 1986.
2. Petkovich, M., Brand, N.J., Krust, A., Chambon, P. A human retinoic acid receptor which belongs to the family of nuclear receptors. Nature 330:444–450, 1987.
3. Giguere, V., Ong, E.S., Segui, P., Evans, R.M. Identification of a receptor for the morphogen retinoic acid. Nature 330:624–629, 1987.
4. Ronne, H., Ocklind, C., Wiman, K., Rask, L., Öbrink, B., Peterson, P.A. Ligand-dependent regulation of intracellular protein transport: Effect of vitamin A on the secretion of the retinol binding protein. J. Cell Biol. 96:907–910, 1983.
5. Goodman, D.S. Plasma retinol binding proteins. In: "The Retinoids," Vol. 2. Sporn, M.B., Roberts, A.B., Goodman, D.S. (eds.). New York: Academic Press, 1984:41–88.
6. Kanai, M., Raz, A., Goodman, D.S. Retinol binding protein: The transport protein for vitamin A in human plasma. J. Clin. Invest. 47:2025–2044, 1968.
7. Rask, L., Anundi, H., Böhme, J., Eriksson, U., Fredriksson, Å., Nilsson, S.F., Ronne, H., Vahlquist, A., Peterson, P.A. The retinol binding protein. Scand. J. Clin. Lab. Invest. 40:45–61, 1980.
8. Newcomer, M.E., Jones, T.A., Åqvist, J., Sundelin, J., Eriksson, U., Rask, L., Peterson, P.A. The three-dimensional structure of retinol-binding protein. EMBO J. 3: 1451–1454, 1984.
9. Pervaiz, S., Brew, K. Homology of β-lactoglobulin, serum retinol-binding protein, and protein HC. Science 228: 335–337, 1985.
10. Papiz, M.Z., Sawyer, L., Eliopoulos, E.E., North, A.C.T., Findlay, J.B.C., Sivaprasadarao, R., Jones, T.A., Newcomer, M.E., Kraulis, P.J. The structure of β-lactoglobulin and its similarity to plasma retinol binding protein. Nature 324:383–385, 1986.
11. Pevsner, J., Reed, R.R., Feinstein, P.G., Snyder, S.H. Molecular cloning of odorant-binding protein: Member of a ligand carrier family. Science 241:336–339, 1988.
12. Sawyer, L. One fold among many. Nature 327:659–659, 1987.
13. Godovac-Zimmermann, J. The structural motif of β-lactoglobulin and retinol binding protein: A basic framework for binding and transport of small hydrophibic molecules. TIBS 13:64–66, 1988.
14. Sawyer, L., Papiz, M.Z., North, A.C.T., Eliopoulos, E.E. Structure and function of bovine β-lactoglobulin. Biochem. Soc. Trans. 13:265–266, 1985.
15. Monaco, H.L., Zanotti, G., Spadon, P., Bolognesi, M., Sawyer, L., Eliopoulos, E.E. Crystal structure of the trigonal form of bovine β-lactoglobulin and its complex with retinol at 2.5 Å resolution. J. Mol. Biol. 197:695–706, 1987.
16. Huber, R., Schneider, M., Epp, O., Mayr, I., Messerschmidt, A., Pfulgrath, J., Kayser, H. Crystallization, crystal structure analysis and preliminary molecular model of the bilin binding protein (BBP) from the insect *Pieris brassicae*. J. Mol. Biol. 195:423–434, 1987.
17. Holden, H.M., Rypniewski, W.R., Law, J.H., Rayment, I. The molecular structure of insecticyanin from the tobacco hornworm *Manduca sexta*. 1. at 2.6 Å resolution. EMBO J. 6:1565–1570, 1987.
18. Huber, R., Schneider, M., Mayr, I., Müller, R., Deutzmann, R., Suter, F., Zuber, H., Falk, H., Kayser, H. Molecular structure of the bilin binding protein (BBP) from *Pieris brassicae* after refinement at 2.0 Å resolution. J. Mol. Biol. 198:499–513, 1987.
19. Chytil, F., Ong, D.E. Cellular retinoid-binding proteins. In: "The Retinoids," Vol. 2. Sporn, M.B., Roberts, A.B., Goodman, D.S. (eds.). New York: Academic Press, 1984: 89–123.
20. Li, E., Demmer, L.A., Sweetser, D.A., Ong, D.E., Gordon, J.I. Rat cellular retinol binding protein II: Use of a cloned cDNA to define its primary structure, tissue-specific expression, and developmental regulation. Proc. Natl. Acad. Sci. USA 83:5779–5783, 1986.
21. Bashor, M.M., Toft, D.O., Chytil, F. In vitro binding of retinol to rat-tissue components. Proc. Natl. Acad. Sci. USA 70:3483–3487, 1973.
22. Sani, B.P., Hill, D.L. Retinoic acid: A binding protein in chick embryo metatarsal skin. Biochem. Biophys. Res. Commun. 61:1276–1282, 1974.
23. Sundelin, J., Dass, S.R., Eriksson, U., Rask, L., Peterson, P.A. The primary structure of bovine cellular retinoic acid-binding protein. J. Biol. Chem. 260:6494–6499, 1985.
24. Jones, T.A., Bergfors, T., Sedzik, J., Unge, T. The three-dimensional structure of P2 myelin. EMBO J. 7:1597–1604, 1988.
25. Sacchettini, J.C., Gordon, J.I., Banaszak, L.J. The structure of crystalline *Escherichia coli*-derived rat intestinal fatty acid-binding protein at 2.5 Å resolution. J. Biol. Chem. 263:5815–5819, 1988.
26. Peterson, P.A., Berggård, I. Isolation and properties of a human retinol-transporting protein. J. Biol. Chem. 246: 25–33, 1971.
27. Newcomer, M.E., Liljas, A., Sundelin, J., Rask, L., Peterson, P.A. Crystallization of and preliminary x-ray data for the plasma retinol binding protein. J. Biol. Chem. 259:5230–5231, 1984.
28. Eklund, H., Nordström, B., Zeppezauer, E., Söderlund, G., Ohlsson, I., Boiwe, T., Söderberg, B.-O., Tapia, O., Brändén, and C.-I., Åkeson, Å. Three-dimensional structure of horse liver alcohol dehydrogenase at 2.4 Å resolution. J. Mol. Biol. 102:27–59, 1976.
29. Franks, A. An optically focusing x-ray diffraction camera. Proc. Phys. Soc. B68:1054–1064, 1955.
30. Rossmann, M.G. Processing oscillation diffraction data for very large unit cells with an automatic convolution technique and profile fitting. J. Appl. Cryst. 12:225–238, 1979.
31. Dickerson, R.E., Kendrew, J.C., Strandberg, B.E. The crystal structure of myoglobin: Phase determination to a resolution of 2 Å by the method of isomorphous replacement. Acta Cryst. 14:1188–1195, 1961.
32. Blow, D.M., Crick, F.H.C. The treatment of errors in the isomorphous replacement method. Acta Cryst. 12:794–802, 1959.
33. Jones, T.A. A graphics model building and refinement system for macromolecules. J. Appl. Cryst. 11:268–272, 1978.
34. Jones, T.A. FRODO: A graphics fitting program for macromolecules. In: "Computational Crystallography." Sayre, D. (ed.). Oxford: Clarendon Press, 1982:303–317.
35. Sussman, J.L., Holbrook, S.R., Church, G.M., Kim, S.-H. A structure-factor least-squares refinement procedure for macromolecular structures using constrained and restrained parameters. Acta Cryst. A33:800–804, 1977.
36. Hendrickson, W.A., Konnert, J.H. Incorporation of stereochemical information into crystallographic refinement. Computing in crystallography. Indian Acad. Sci. 13.01–13.25, 1980.
37. Brünger, A.T., Kuriyan, J., Karplus, M. Crystallographic R factor refinement by molecular dynamics. Science 235: 458–460, 1987.

38. Rask, L., Anundi, H., Peterson, P.A. The primary structure of the human retinol-binding protein. FEBS Lett. 104:55–58, 1979.
39. Ramakrishnan, C., Ramachandran, G.N. Stereochemical criteria for polypeptide and protein chain conformation. Biophys. J. 5:909–933, 1965.
40. Balasubramanian, R. New type of representation for mapping chain-folding in protein molecules. Nature 266: 856–857, 1977.
41. Kabsch, W., Sander, C. Dictionary of protein secondary structure: Pattern recognition of hydrogen-bonded and geometrical features. Biopolymers 22:2577–2637, 1983.
42. Efimov, A.V. Standard conformations of a polypeptide chain in irregular protein regions. Mol. Biol. (Mosk.) 20: 250–260, 1986.
43. Sundelin, J., Laurent, B.C., Anundi, H., Trägårdh, L., Larhammar, D., Björck, L., Eriksson, U., Åkerström, B., Jones, A., Newcomer, M., Peterson, P.A., Rask, L. Amino acid sequence homologies between rabbit, rat, and human serum retinol binding proteins. J. Biol. Chem. 260: 6472–6480, 1985.
44. Chothia, C., Janin, J. Orthogonal packing of β-pleated sheets in proteins. Biochemistry 21:3955–3965, 1982.
45. Richardson, J.S. The anatomy and taxonomy of protein structure. Adv. Protein Chem. 34:167–339, 1981.
46. Sibanda, B.L., Thornton, J.M. β-hairpin families in globular proteins. Nature 316:170–174, 1985.
47. Bolin, J.T., Filman, D.J., Matthews, D.A., Hamlin, R.C., Kraut, J. Crystal structures of *Escherichia coli* and *Lactobacillus casei* dihydrofolate reductase refined at 1.7Å resolution. I. General features and binding of methotrexate. J. Biol. Chem. 257:13650–13662, 1982.
48. Chothia, C. Principles that determine the structure of proteins. Annu. Rev. Biochem. 53:537–572, 1984.
49. Rask, L., Anundi, H., Böhme, J., Eriksson, U., Ronne, H., Sege, K., Peterson, P.A. Structural and functional studies of vitamin A-binding proteins. Ann. NY Acad. Sci. 359: 79–90, 1981.
50. Colantuoni, V., Romano, V., Bensi, G., Santoro, C., Costanzo, F., Raugei, G., Cortese, R. Cloning and sequencing of a full length cDNA coding for human retinol binding protein. Nucleic Acids Res. 11:7769–7776, 1983.
51. Lee, B., Richards, F.M. The interpretation of protein structures: Estimation of static accessibility. J. Mol. Biol. 55:379–400, 1971.
52. Jones, T.A., Liljas, L. Structure of satellite tobacco necrosis virus after crystallographic refinement at 2.5 Å resolution. J. Mol. Biol. 177:735–767, 1984.
53. Peterson, P.A. Characteristics of a vitamin A-transporting protein complex occuring in human serum. J. Biol. Chem. 246:34–43, 1971.
54. Goodman, D.S., Rax, A. Extraction and recombinant studies of the interaction of retinol with human plasma retinol binding protein. J. Lipid Res. 13:338–347, 1972.
55. Horwitz, J., Heller, J. Interactions of all-trans-,9,11-, and 13-cis-retinal, all-transretinyl acetate, and retinoic acid with human retinol binding protein and prealbumin. J. Biol. Chem. 248:6317–6324, 1973.
56. Cogan, U., Kopelman, M., Mokady, S., Shinitzky, M. Binding affinities of retinol and related compounds to retinol binding proteins. Eur. J. Biochem. 65:71–78, 1976.
57. Hase, J., Kobashi, K., Nakai, N., Onosaka, S. Binding of retinol binding protein obtained from human urine with vitamin A derivates and terpenoids. J. Biochem. 79:373–380, 1976.
58. Gawinowicz, M.A., Goodman, D.S. Retinoid affinity label for the binding site of retinol binding protein. Biochemistry 21:1899–1905, 1982.
59. Gawinowicz, M.A., Goodman, D.S. The site of linkage of a retinoid affinity label to plasma retinol binding protein. J. Protein Chem. 4:199–213, 1985.
60. Ottonello, S., Maraini, G., Mammi, M., Monaco, H.L., Spadon, P., Zanotti, G. Crystallization and preliminary x-ray data of human plasma retinol binding protein. J. Mol. Biol. 163:679–681, 1983.
61. Monaco, H.L., Zanotti, G., Ottonello, S., Berni, R. Crystallization of human plasma aporetinol binding protein. J. Mol. Biol. 178:477–479, 1984.
62. Horwitz, J., Heller, J. Conformational changes following interaction between retinol isomers and human retinol binding protein and between the retinol-binding protein and prealbumin. J. Biol. Chem. 248:6308–6316, 1973.
63. Peterson, P.A. Demonstration in serum of two physiological forms of the human retinol binding protein. Eur. J. Clin. Invest. 1:437–444, 1971.
64. Fex, G., Albertsson, P.-Å., Hansson, B. Interaction between prealbumin and retinol binding protein studied by affinity chromatography, gel filtration and two-phase partition. Eur. J. Biochem. 99:353–360, 1979.
65. Raz, A., Goodman, D.S. The interaction of thyroxine with human plasma prealbumin and with the prealbumin-retinol-binding protein complex. J. Biol. Chem. 244: 3230–3237, 1969.
66. Rask, L., Vahlquist, A., Peterson, P.A. Studies on two physiological forms of the human retinol binding protein differing in vitamin A and arginine content. J. Biol. Chem. 246:6638–6646, 1971.
67. Horwitz, J., Heller, J. Modification of tryptophan residues in retinol binding protein and prealbumin with 2-hydroxy-5-nitrobensyl bromide. J. Biol. Chem. 249:7181–7185, 1974.
68. Kopelman, M., Cogan, U., Mokady, S., Shinitzky, M. The interaction between retinol binding proteins and prealbumins studied by fluorescence polarization. Biochim. Biophys. Acta 439:449–460, 1976.
69. Åqvist, J., Sandblom, P., Jones, T.A., Newcomer, M.E., van Gunsteren, W.F., Tapia, O. Molecular dynamics simulations of the holo and apo forms of retinol binding protein. J. Mol. Biol. 192:593–604, 1986.
70. Peterson, P.A. Studies on the interaction between prealbumin, retinol binding protein, and vitamin A. J. Biol. Chem. 246:44–49, 1971.
71. Dayhoff, M., Barker, W.C., Hunt, L.T. Establishing homologies in protein sequences. Methods Enzymol. 91: 524–545, 1983.
72. Godovac-Zimmerman, J., Conti, A., Liberatori, J., Braunitzer, G. Homology between the primary structures of β-lactoglobulins and human retinol-binding protein: Evidence for a similar biological function? Biol. Chem. Hoppe Seyler 366:431–434, 1985.
73. Berman, P., Gray, P., Chen, E., Keyser, K., Ehrlich, D., Karten, H., LaCorbiere, M., Esch, F., Schubert, D. Sequence analysis, cellular localization, and expression of a neuroretina adhesion and cell survival molecule. Cell 51: 135–142, 1987.
74. Riley, C.T., Barbeau, B.K., Keim, P.S., Kézdy, F.J., Heinrikson, R.L., Law, J.H. The covalent protein structure of insecticyanin, a blue biliprotein from the hemolymph of the tobacco hornworm, *Manduca sexta* L. J. Biol. Chem. 259:13159–13165, 1984.
75. Braunitzer, G., Chen, R., Schrank, B., Stangl, A. Die sequenzanalyse des β-lactoglobulins. Hoppe Seylers Z. Physiol. Chem. 354:867–878, 1973.
76. Futterman, S., Heller, J. The enhancement of fluorescence and the decreased susceptibility to enzymatic oxidation of retinol complexed with bovine serum albumin, β-lactoglobulin, and the retinol-binding protein of human plasma. J. Biol. Chem. 247:5168–5172, 1972.
77. Drayna, D., Fielding, C., McLean, J., Baer, B., Castro, G., Chen, E., Comstock, L., Henzel, W., Kohr, W., Rhee, L., Wion, K., Lawn, R. Cloning and expression of human apolipoprotein D cDNA. J. Biol. Chem. 261:16535–16539, 1986.
78. Ekström, B., Peterson, P.A., Berggård, I. A urinary and plasma α1-glycoprotein of low molecular weight: Isolation and some properties. Biochem. Biophys. Res. Commun. 65:1427–1433, 1975.
79. Lopez, C., Grubb, A., Soriano, F., Mendez, E. The complete amino acid sequence of human complex-forming glycoprotein heterogenous in charge (protein HC). Biochem. Biophys. Res. Commun. 103:919–925, 1981.
80. Brooks, D.E., Means, A.R., Wright, E.J., Singh, S.P., Tiver, K.K. Molecular cloning of the cDNA for two major androgen-dependent secretory proteins of 18,5 kilodaltons synthesized by the rat epididymis. J. Biol. Chem. 26:4956–4961, 1986.
81. Dolan, K.P., Unterman, R., McLaughlin, M., Nakhasi, H.L., Lynch, K.R., Feigelson, P. The structure and ex-

pression of very closely related members of the α2μ-globulin gene family. J. Biol. Chem. 257:13527–13534, 1982.
82. Clark, A.J., Clissold, P.M., Al Shaw, R., Beattie, P., Bishop, J. Structure of mouse major urinary protein genes: Different splicing configurations in the 3'-non-coding region. EMBO J. 3:1045–1052, 1984.
83. Ricca, G.A., Taylor, J.M. Nucleotide sequence of rat α_1-acid glycoprotein messenger RNA. J. Biol. Chem. 256: 11199–11202, 1981.
84. Lee, K.H., Wells, R.G., Reed, R.R. Isolation of an olfactory cDNA: Similarity to retinol-binding protein suggests a role in olfaction. Science 235:1053–1056, 1987.
85. Julkunen, M., Seppälä, M., Jänne, O.A. Complete amino acid sequence of human placental protein 14: A progesterone-regulated uterine protein homologous to β-lactoglobulins. Proc. Natl. Acad. Sci. USA 85:8845–8849, 1988.
86. Henzel, W.J., Rodriguez, H., Singer, A.G., Stults, J.T., Macrides, F., Agosta, W.C., Niall, H. The primary structure of aphrodisin. J. Biol. Chem. 263:16682–16687, 1988.
87. Schmid, K. In: "The Plasma Proteins," Vol. I. Putnam, F. (ed.). New York: Academic Press, 1975:184–228.
88. Murthy, M.R., Reid, T.J., Sicignano, A., Tanaka, N., Rossmann, M.G. Structure of beef liver catalase. J. Mol. Biol. 152:465–499, 1981.
89. Hendrickson, W.A., Pähler, A., Smith, J.L., Satow, Y., Merritt, E.A., Phizackerley, R.P. Crystal structure of core streptavidin determined from multiwavelength anomalous diffraction of synchrotron radiation. Proc. Natl. Acad. Sci. USA 86:2190–2194, 1989.
90. Weber, P.C., Ohlendorf, D.H., Wendoloski, J.J., Salemme, F.R. Structural origins of high-affinity biotin binding to streptavidin. Science 243:85–88, 1989.
91. McRee, D.E., Tainer, J.A., Meyer, T.E., Van Beeumen, J., Cusanovich, M.A., Getzoff, E.D. Crystallographic structure of a photoreceptor protein at 2.4Å resolution. Proc. Natl. Acad. Sci. USA 86:6533–6537, 1989.
92. Thackeray, M.M., Gafner, G. The crystal structure of 2,6-di-cis-4-hydroxyretinoic acid γ-lactone. Acta Cryst. B31: 335–338, 1975.
93. Stam, C.H. The crystal structure of a monoclinic modification and the refinement of a triclinic modification of vitamin A acid (retinoic acid), $C_2OH_{28}O_2$. Acta. Cryst. B28:2936–2945, 1972.
94. Gilardi, R.D., Karle, I.L., Karle, J. The crystal and molecular structure of 11-cis-retinal. Acta Cryst. B28:2605–2612, 1972.
95. Thackeray, M.M., Gafner, G. The crystal structure of 2-cis-4-hydroxyretinoic acid γ-lactone. Acta Cryst. B30: 1711–1714, 1974.
96. Oberhänsli, W.E., Wagner, H.P., Isler, O. The crystal structure of vitamin A acetate. Acta Cryst. B30:161–166, 1974.
97. Hamanaka, T., Mitsui, T., Ashida, T., Kakudo, M. The crystal structure of all-trans retinal$_1$. Acta. Cryst. B28: 214–222, 1972.
98. Simmons, C.J., Liu, R.S.H., Denny, M., Seff, K. The crystal structure of 13-cis-retinal. The molecular structure of its 6-s-cis and 6-s-trans conformers. Acta Cryst. B37: 2197–2205, 1981.
99. Schenk, H., Kops, R.T., van der Putten, N., Bode, J. The structure of the 9-ethyl analogue of vitamin A acid. Acta Cryst. B34:505–507, 1978.
100. Priestle, J.P. RIBBON: A stereocartoon drawing program for proteins. J. Appl. Cryst. 21:572–576, 1988.